

Supporting Information for

Substrate Tolerant Direct Block Copolymer Nanolithography

Tao Li, Zhongli Wang, Lars Schulte, Sokol Ndoni.

This file includes:

Experimental section

Figures S1 to S6

Discussion of solvent vapor annealing conditions

Chart S1, Figure S7

Tables S1 to S5

References (1-6)

Experimental section:

Synthesis: All the solvents are purchased from Sigma Aldrich without further purification (except for the BC synthesis). SD67 (21-b-46 kg mol⁻¹, Polymer Source), PS (50k, synthesized in our lab), PMMA (70k, Diakon), PSF (27k, Scientific Polymers), PLA (M_w 18k-28k, Sigma Aldrich), PB (Scientific Polymers, MW 100k, crosslinking procedure:¹) and monolayer Graphene on SiO₂/Si (Graphenea) are used as received. SD42, SD34 and SD23 are synthesized by living anionic polymerization following already reported procedure.² After precipitation in methanol and vacuum drying, SD is dissolved in heptane (5wt %). Clear solutions are obtained in heptane, despite the fact that it is a nonsolvent for PS; the SDs most probably form micelles in such conditions. However, the solutions turn turbid after a residence time of 10-20 hours, and the undissolved solids are removed by centrifugation. This step is essential for a reliable following self-assembly process, since we find that even a small amount of unreacted PS impurity makes the whole process less robust. Size exclusion chromatography (SEC) traces of the supernatant are indistinguishable from the SEC of the as synthesized SDs (except for SD34, see below), which is consistent with less than 1% of precipitated mass fraction. As synthesized SD34 shows a little but distinguishable SEC peak of uncoupled PS, which is significantly diminished after fractionation in heptane (data not shown). Most probably the PS homopolymer seeds the formation of large SD cylindrical micelles that can be removed by centrifugation. Then the supernatant is diluted in heptane at 0.12 -0.28 wt %, giving films with thickness from 12 nm to 20 nm at spinning speed of 2000 rpm.

Fabrication: Solvent vapor annealing is made at room temperature with the samples in a closed glass jar in the presence of chosen annealing solvent(s). The annealing time is typically up to 1

hour. Using solvents that are strongly selective to PDMS effectively prevents dewetting since the mobility of the PS block is limited, resulting in a highly controlled and reproducible process. No dewetting is observed for this study; however, using neutral solvents like toluene causes substrate dewetting in less than 2 minutes. The annealing solvents are nonsolvents for PS; however given the structural rearrangement observed these are able to slightly swell the PS block by bringing it in the rubbery state. The swelling ratio of a 10 nm PS film is measured to 1.2 – 1.24 at 40 – 75 min hexane vapor annealing time by a quartz crystal microbalance, QCM (see below). This degree of swelling is compatible with literature reports on PS glass transition temperature T_g decrease below room temperature.³

The dry etch process is performed on an Advanced Silicon Etcher (STS MESC Multiplex ICP serial no. 30343). SF₆ plasma condition for pretreatment: 20 sccm SF₆, 20 mTorr, coil power: 50w and platen power: 0w, 5 – 10 seconds. O₂ plasma condition for the pattern transfer: 10 sccm O₂, 5 mTorr, coil power: 200w and platen power: 20w. SF₆ plasma condition for mask removal: 50 sccm SF₆, 20 mTorr, coil power: 200w and platen power: 2w, 20 seconds. The silicon etching is performed on ICP Metal etch (SPTS Serial number MP0637). Breakthrough step: 20 sccm SF₆, 3 mTorr, coil power: 100w and platen power: 10w, 30 seconds. Cl₂ etching: 20 sccm Cl₂, 3 mTorr, coil power: 400w and platen power: 40w, 90 seconds.

Characterization: ¹H-NMR is done in deuterated chloroform, using a 400 MHz NMR from Bruker. The SEC is done using THF as a solvent. The system from Shimadzu, LC-10AD (Pump), SIL-10AS (Autosampler), is combined with Detectors from Viscotek, namely a RALLS Detector (Model LD600) as well as a Differential Refractometer/Viscometer (Model 200) combination. The columns are: one PLgel 5 μ m Mixed D from Polymer Laboratories in series with one Styragel HMW 6E from Waters. The PS block of the polymers is analyzed using the Refractive

Index signal in combination with a conventional calibration against PS standards, while calculations of PDI for the BCs, is done by analyzing the combined Light Scattering and Refractive Index responses. Film thickness is determined by a VASE Ellipsometer (J.A. Woollam) at three different incidence angles (55°, 60° and 65°). Scanning electron microscopy (SEM) images are taken by a Field Emission Zeiss Ultra Plus scanning electron microscope with a Gemini column operating at an accelerating voltage of 2kV. The cross-section is taken at a tilt angle of 45°. All the samples are imaged directly without coating or staining. Atomic Force Microscopy (AFM) images are taken by an AFM Dimension Icon-PT from Bruker AXS. A Thermo DXR-Raman system with a laser wavelength of 455 nm is used for the characterization of graphene samples. The resolution is 5.9 – 8.5 cm⁻¹, spot size is 0.5 μm, collect exposure time is 10 s per scan, and 8 scans are accumulated for each sample. XPS measurement is performed on a XPS-ThermoScientific instrument. The annealing process is followed in situ by a quartz crystal microbalance QCM 200 digital controller connected to a QCM 25 crystal oscillating at 5 MHz from Stanford Research Systems. The block copolymer or PS 50k are spin-cast directly on the quartz crystal with a gold electrode at same conditions as for the sample preparation on the different substrates. An accuracy of better than 1 Hz, corresponding to mass differences of smaller than 0.017 μg/cm² or film height changes of ~ 2 Å is routinely achieved.

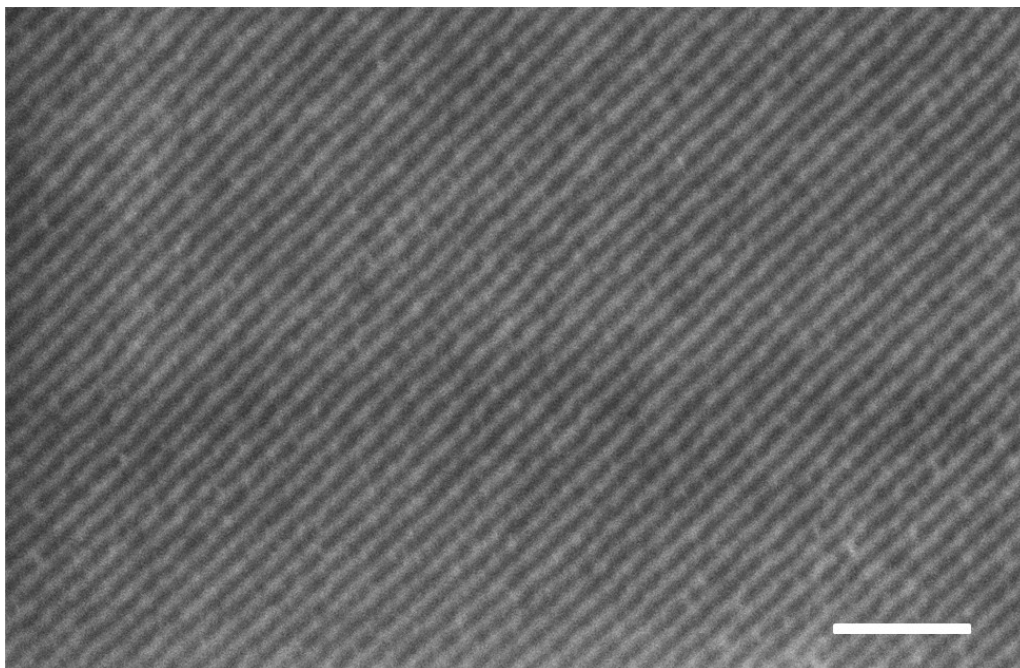


Figure S1. SEM image of the bulk morphology of SD23 (600 nm thick film on silicon wafer), annealed at 160°C for 20 hours. The image is taken after 200 nm top layer removal by SF_6/O_2 RIE. The observed period is 29 nm and is equal to the characteristic distance between two cylinders. The corresponding period is 24 nm, which is slightly bigger than the period of thin film cylinder morphology (table S1). Scale bar: 200 nm.

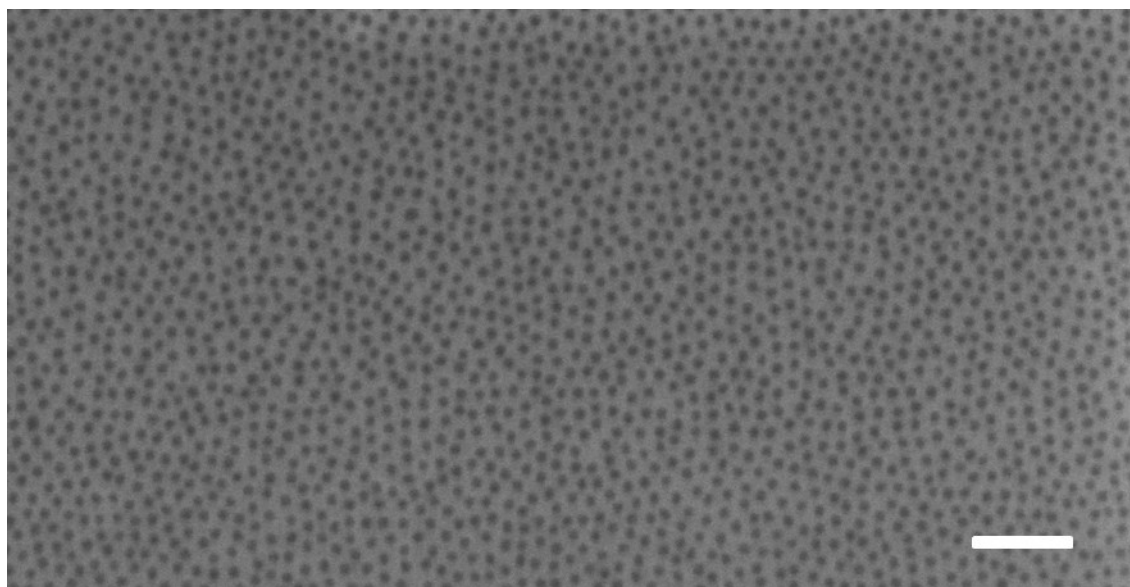


Figure S2. SEM image of the SD67 annealed in 1-octene for 1 hour. Scale bar: 200nm. The lacking in lateral order might be due to its large PDI.

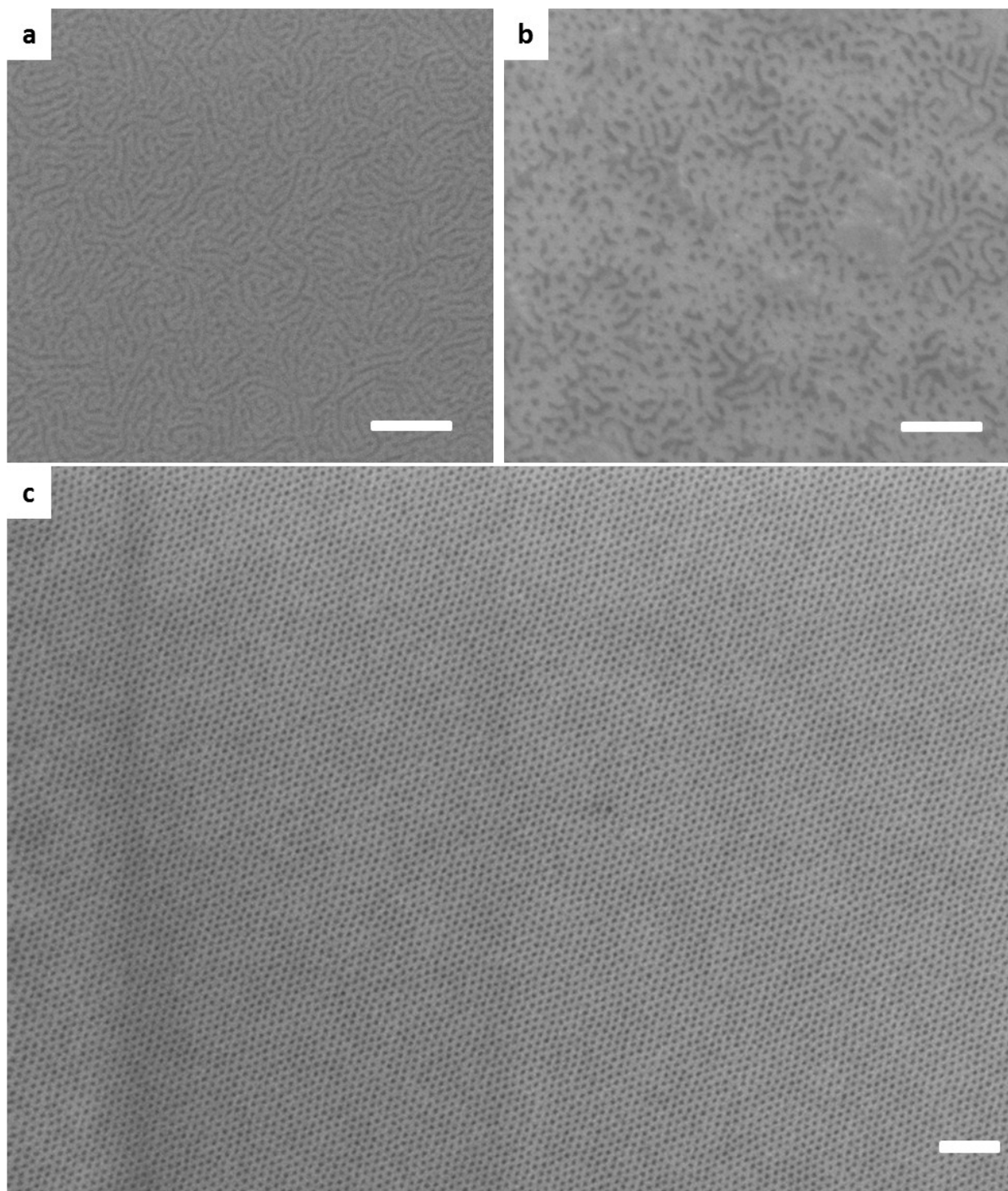


Figure S3. SEM image of the SD42 as cast on PS substrate a); the shown morphology is similar for all the SDs after spin-casting, b) SD42 thermal annealed at 160°C for 15 hours and c) SD42 annealed in hexane for 40 minutes with the grain size exceeding 4 μm . Scale bars: 200 nm.

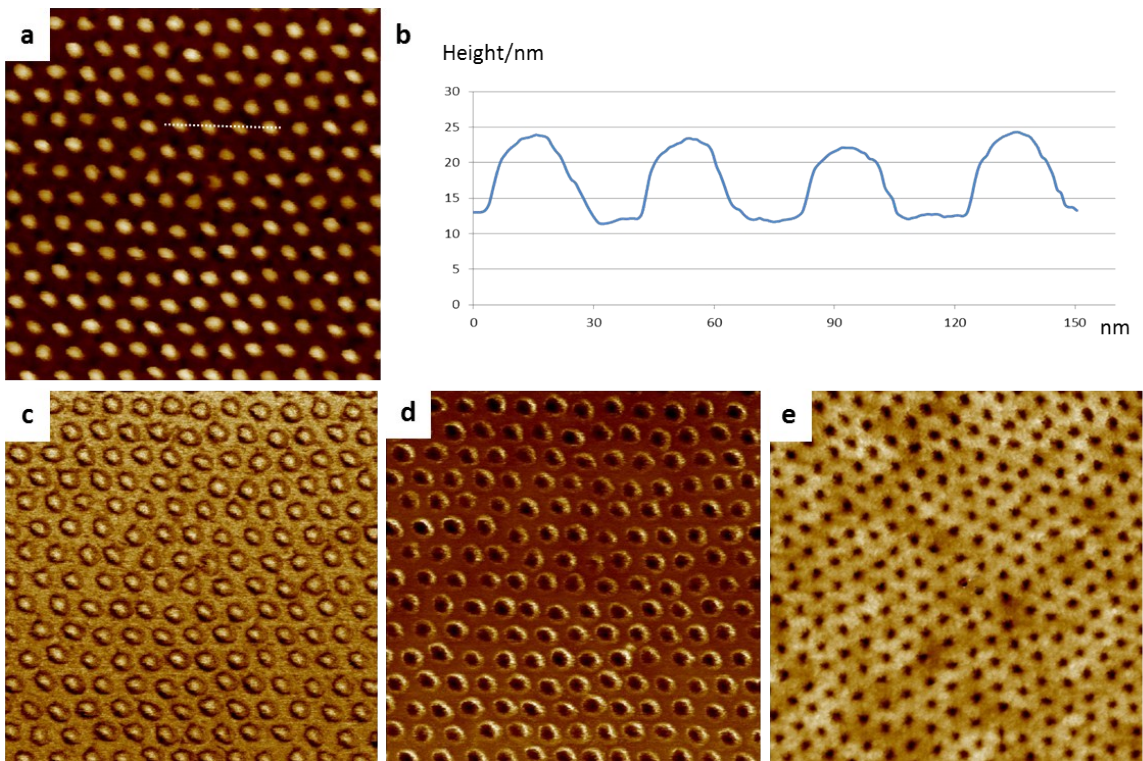


Figure S4. AFM image of the SD42 annealed in hexane for 40 minutes: a) height mode, b) section profile of (a), c) modulus mode, d) adhesion mode and e) height mode after etching; size: 500nm x 500nm.

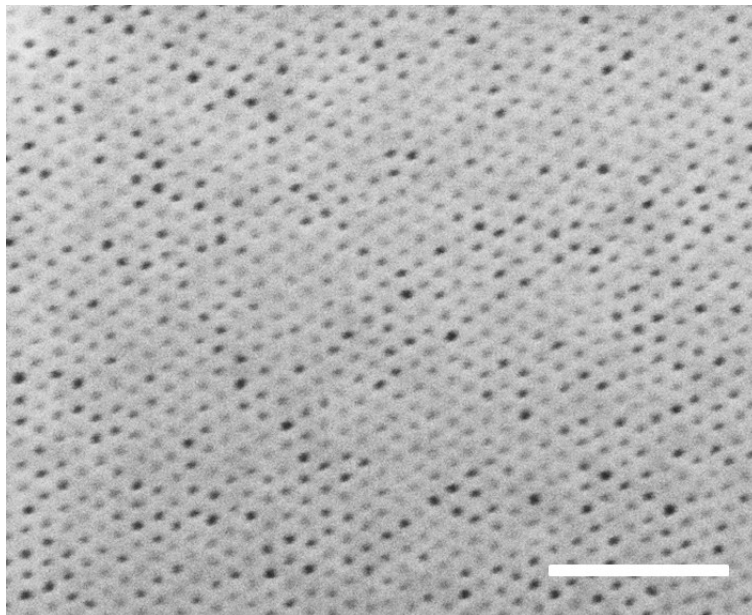


Figure S5. SEM image of the SD23 on PS substrate after O₂ RIE. Scale bar: 200nm.

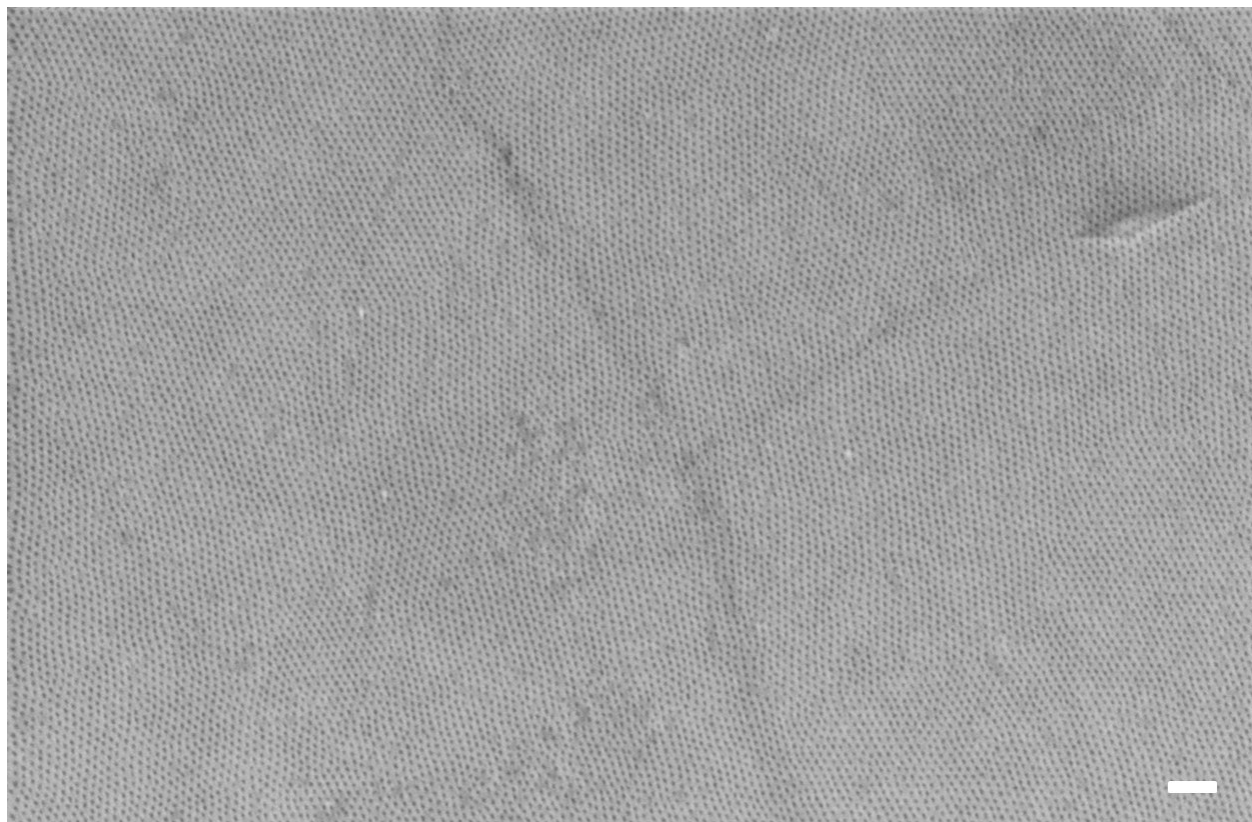


Fig. S6. SEM image of the SD42 directly cast on graphene substrate, and annealed in hexane for 10 minutes. Scale bar: 200nm.

Discussion of solvent vapor annealing conditions

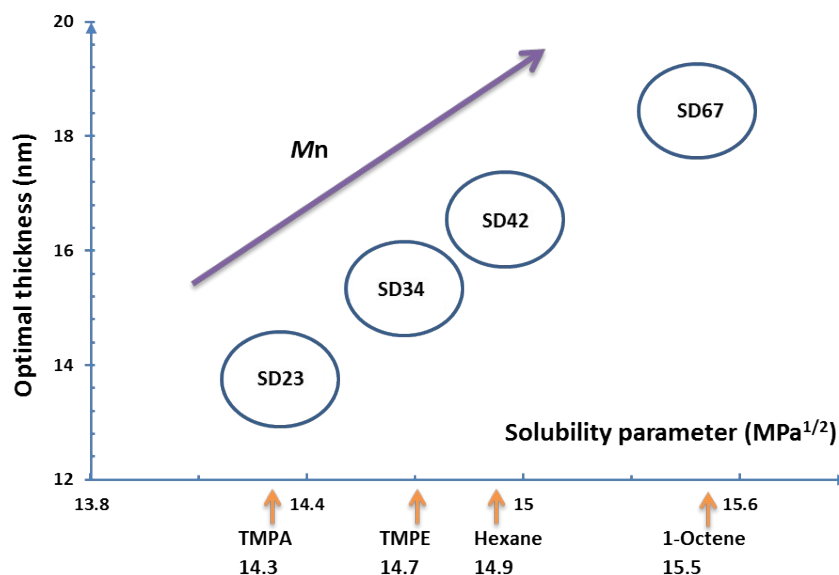


Chart S1. Processing window for the film thickness and annealing conditions. The optimum processing space ranges of film thicknesses and solvent solubility parameters shown by the bubbles do not have clean-cut boundaries. However, we experience readily induced defects when operating outside the shown optimum zones (Figure S7, supporting information).

The interaction between solvent and polymer can be considered in terms of Hildebrand solubility parameters (Table S4, supporting information). Chart S1 summarizes the optimum annealing conditions for each SD. There is a clear trend between the film thickness and the solubility parameter of the annealing selective solvent appropriate for each SD molecular weight. The optimum film thicknesses slightly exceed half respective structural periods for the first three SD samples, or roughly $3R_g$, where R_g stands for the radius of gyration of the respective block copolymer chains. In addition to the solvents listed in Chart S1 for each SD, other solvents with similar solubility parameters or mixed solvents (Table S5, supporting information) are effective as well. There is at least a 30 minutes processing window where the defect-free morphology can be captured for each SD on a PS substrate, which qualifies the method as well-defined and reliable. This guideline can be used as a powerful tool to predict suitable annealing conditions for SD with similar composition and different molecular weights.

The vapor annealing process is monitored in situ by quartz crystal microbalance (QCM) measurements; the obtained swelling data support that (1) the SD samples are in the microphase

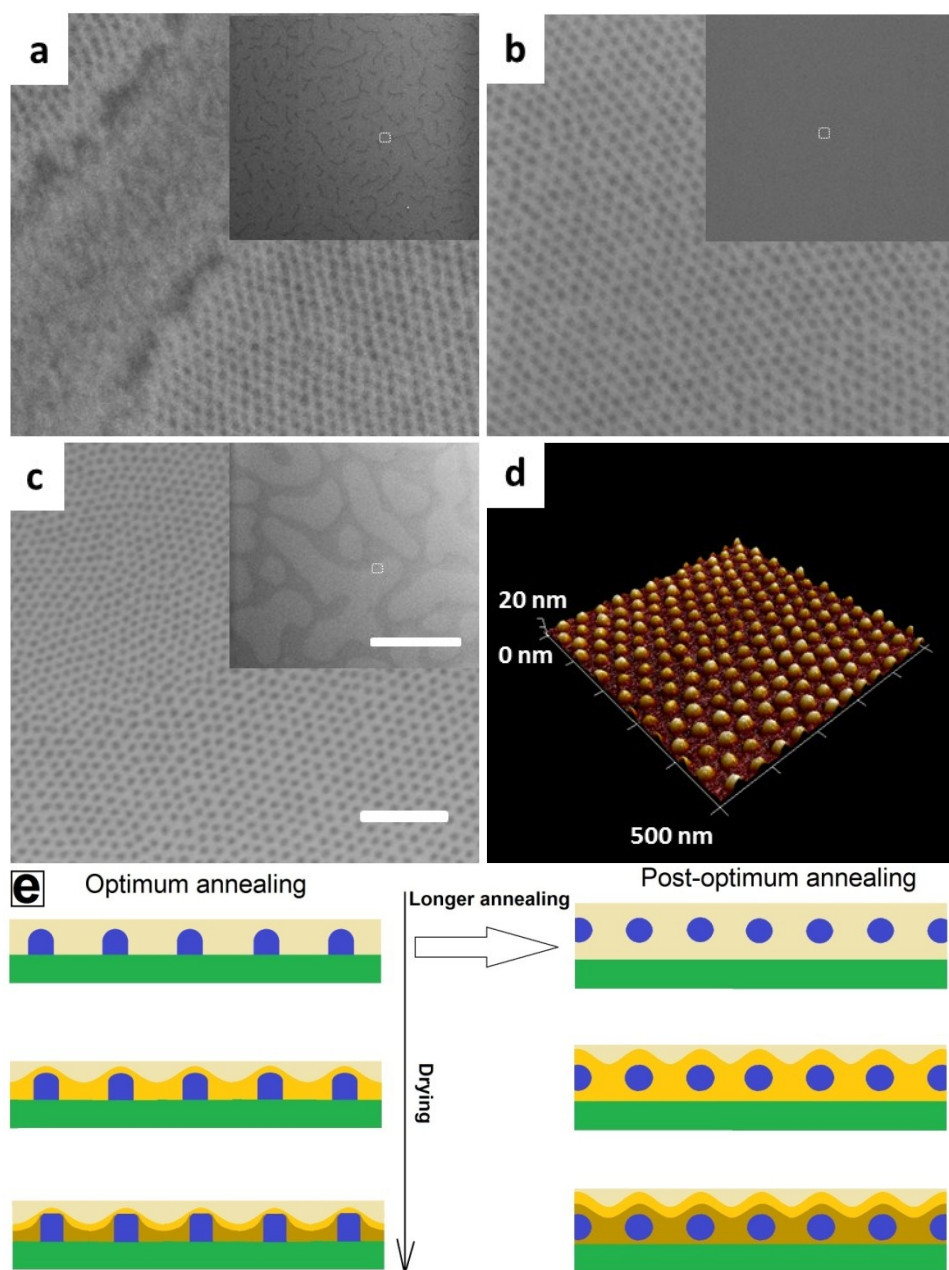


Figure S7. Images of the SD42 morphology evolution. Top view SEM images of SD42 annealed in hexane for (a) 15 minutes; (b) between 20 and 60 minutes; (c) 75 minutes. The main pictures in frames (a-c) are high magnification images of the regions delimited by the little squares in the respective insets; (d) 3D rendering of the AFM image in Figure S4. Scale bars: 200 nm and 20 μm (insets). (e) Schematics of the proposed mechanism for structure formation at and beyond the optimum annealing window. The darker yellow-brown color represents lower solvent content. Over the entire optimum annealing window the structure in the swollen state consists of hexagonally packed half-spherical or half-sphere capped cylindrical PS domains swollen by a factor of approx. 1.2 surrounded by PDMS coronae swollen by estimated factors of 1.5 – 1.7. At post-optimum annealing the observed morphology shown in panel (c) is consistent with domains of cylinders (lower part of fig. S7c) confined by developing domains of spheres

(upper part in the same figure). The cylinder (sphere) domains appear as light (dark) regions in the low magnification insert image of fig. S7c. The structure transition from cylinders to spheres is schematically depicted in panel S7e.

segregated state during annealing, and (2) the PDMS domains are 2.5-3 times more swollen than the PS domains. The effective volume fraction of the PS block f_S in SD42 varies from 0.29 in the dry state to 0.24, 0.23, 0.22 after resp. 40, 60, 75 min of hexane vapor annealing time. At f_S of approx. 0.22 – 0.24 self-consistent field calculations⁴ predict cylinder to sphere order-to-order transition in the thin film regime. However, the model in ref. 4 assumes symmetrical interfacial potential and absence of solvent, which are both not satisfied by our system. The solid surface is preferential to PS and air is preferential to PDMS. Therefore the model is not expected to describe our system quantitatively. Indeed, the model predicts laying cylinders or hexagonally perforated lamellae as stable morphologies at $f_S = 0.24$ and film thickness $w = 3R_g$, similar to ours, R_g being the radius of gyration of an unperturbed SD macromolecule. Stable standing cylinder morphologies are predicted at film thicknesses below $2R_g$. These discrepancies could be clarified by more realistic, and complex, models of solvent vapor annealing process in the future.

Table S1. PS-b-PDMS Copolymer Characteristics

Sample ID	f_{PS}	M_{PS} (kg/mol)	M_{Total} (kg/mol)	PDI	Periodicity (cylinders) ^f
SD23	28.6% ^a	7.1 ^b	23.4 ^c	1.02 ^e	24 nm
SD34	24.0% ^a	8.7 ^b	34.1 ^c	1.03 ^e	30 nm
SD42	28.6% ^a	12.6 ^b	41.6 ^c	1.02 ^e	33 nm
SD 67	29.7% ^d	21.0 ^d	67.0 ^d	1.45 ^d	45 nm

^aCalculated from ¹H NMR spectra using $\rho_{PDMS} = 0.97 \text{ g/cm}^3$ and $\rho_{PS} = 1.05 \text{ g/cm}^3$.

^bFrom SEC analysis calibrated with PS standards.

^cCalculated from f_{PS} and M_{PS} .

^dFrom the supplier (Polymer Source)

^eFrom SEC analysis of the combined RI and LS signals

^fmeasured from SEM image

$R_g = 4.4 \text{ nm}$ (SD23), 4.9 nm (SD34), 5.7 nm (SD42), 7.2 nm (SD67) [unperturbed conditions, calculated from statistical data, P. J. Flory Statistical Mechanics of Chain Molecules, 1969, Interscience Publ.

Table S2. Condition for SD film free of PDMS top-wetting layer. Only oxygen is needed to transfer the pattern. However to ensure that all the pores are open, we still recommend a short initial fluorine plasma treatment. (HM: Hexamethyldisiloxane and To: Toluene).

BCP	Substrate	Film thickness nm	Annealing solvent*	Anneal time
SD23	PS	13.5	HM/To (20/1)	1 hour
SD42	PS	16.2	Hexane	40 minutes

* Ratio by volume in the liquid phase.

Table S3. Water contact angle measurement

Sample	Angle measured
Si (with native SiO₂ layer)	30
Al₂O₃ by ALD	60
PMMA	65.5
PLA	67
Graphene	69
PSF	73.5
HMDS modified Silicon wafer	80
PS	87
x-linked PB	91
PSF with mask after dry etch	19

Notice from Table S3 that with the exception of cross-linked PB the contact angle does not exceed that of PS. Remembering that the water contact angle of PDMS is $\sim 108^\circ$, one can argue that the PS block should show preferential wetting to the substrates as compared to the PDMS block.

Table S4. Solubility parameters (*)

Solvent	Solubility parameter (MPa^{1/2})
Hexamethyldisiloxane (HM)	12.8
2,2,4-Trimethylpentane (TMPA)	14.3
2,2,3-Trimethylbutane	14.6

2,4,4-Trimethyl-1-pentene (TMPE)	14.7
Hexane	14.9
Heptane	15.2
1-Octene	15.5
Methylcyclohexane	16.2
Toluene	18.2
<i>o</i> -Xylene	18.3
PDMS	15.0 ⁵
PS	18.5 ⁶

(*) Solvent values were calculated from the evaporation enthalpies and molar volumes in ref^[7].

Table S5. Optimal annealing solvent for each BC

BC	Pure solvent	Mixed solvent*
SD23	TMPA, 2,2,3-Trimethylbutane	HM/To (20/1), HM/Xylene (10/1)
SD34	TMPE	HM/To (10/1), HM/Xylene (6/1)
SD42	Hexane, Heptane	HM/To (5/1)
SD67	1-Octene, Methylcyclohexane	Hexane/To (10/1)

*ratio by volume.

References

1. T. Li, L. Schulte, O. Hansen and S. Ndoni, *Micropor Mesopor Mat*, 2015, **210**, 161-168.
2. S. Ndoni, P. Jannasch, N. B. Larsen and K. Almdal, *Langmuir*, 1999, **15**, 3859-3865.
3. J. E. Mark, *Physical properties of polymers handbook*, AIP Press, Woodbury, N.Y., 1996.
4. W. H. Li, M. J. Liu, F. Qiu and A. C. Shi, *J Phys Chem B*, 2013, **117**, 5280-5288.
5. J. E. Mark, *Polymer data handbook*, 2nd edn., Oxford University Press, Oxford ; New York, 2009.
6. K. W. Gotrik, A. F. Hannon, J. G. Son, B. Keller, A. Alexander-Katz and C. A. Ross, *Acs Nano*, 2012, **6**, 8052-8059.
7. C. L. Yaws, *Thermophysical properties of chemicals and hydrocarbons*, Second edition. edn., 2014.